Environmental Science & Technology

Article

pubs.acs.org/est

Dissimilatory Reduction and Transformation of Ferrihydrite-Humic Acid Coprecipitates

Masayuki Shimizu,[†] Jihai Zhou,[†,‡] Christian Schröder,[§] Martin Obst,[∥] Andreas Kappler,[∥] and Thomas Borch*[,†,⊥]

[†]Department of Soil and Crop Sciences, Colorado State University, Fort Collins, Colorado 80523, United States
[‡]School of Environmental and Safety Engineering, Changzhou University, Jiangsu Province, 213164, P. R. China
[§]Biological and Environmental Sciences, School of Natural Sciences, University of Stirling, Stirling FK9 4LA, U.K.
[∥]Center for Applied Geoscience, Eberhard Karls University, 72076 Tuebingen, Germany
[⊥]Department of Chemistry, Colorado State University, Fort Collins, Colorado 80523, United States

Supporting Information

ABSTRACT: Organic matter (OM) is present in most terrestrial environments and is often found coprecipitated with ferrihydrite (Fh). Sorption or coprecipitation of OM with Fe oxides has been proposed to be an important mechanism for long-term C preservation. However, little is known about the impact of coprecipitated OM on reductive dissolution and transformation of Fe(III) (oxyhydr)oxides. Thus, we study the effect of humic acid (HA) coprecipitation on Fh reduction and secondary mineral formation by the dissimilatory Fe(III)-reducing bacterium *Shewanella putrefaciens* strain CN32. Despite similar crystal structure for all coprecipitates investigated, resembling 2-line Fh, the presence of coprecipitated HA resulted in lower specific surface areas. In terms of reactivity, coprecipitated HA resulted in slower Fh bioreduction rates at low C/Fe ratios (i.e., C/Fe ≤ 0.8), while high C/Fe ratios (i.e., C/Fe ≥ 1.8) enhanced the extent of bioreduction compared to pure Fh. The coprecipitated HA also altered the secondary Fe mineralization pathway by inhibiting goethite formation, reducing the amount of magnetite formation, and increasing the formation of a green rust-like phase. This study indicates that coprecipitated OM may influence the rates, pathway, and mineralogy of biogeochemical Fe cycling and anaerobic Fe respiration within soils.

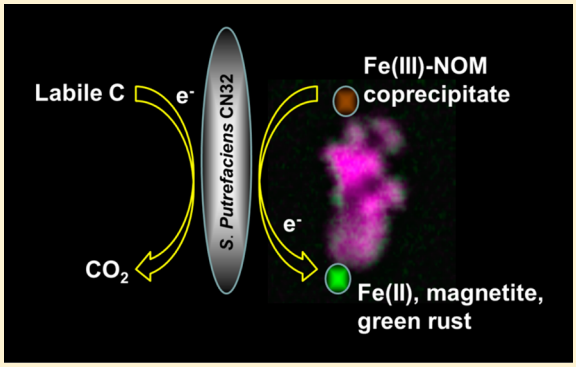

INTRODUCTION

Iron (Fe) is the fourth most abundant element in the Earth's crust, and Fe (oxyhydr)oxide minerals can account for up to 50% of the bulk mass of soils.[1,2] Iron minerals can have large specific surface areas and reactive functional groups, which make them strong sorbents for soil nutrients, contaminants, and organic matter (OM).[3−6] For example, Fe(III) (oxyhydr)-oxides and Al (hydr)oxides are the primary sorbents for arsenic in soils.[7] Unlike Al (hydr)oxides, Fe(III) (oxyhydr)oxides can undergo reductive dissolution in anoxic environments, releasing Fe(II), which may remain in solution, precipitate as secondary Fe(II) or mixed-valence Fe minerals, or become reoxidized to form mixed valence Fe(II/III) or Fe(III) minerals, such as green rust (GR) or Fh via biotic or abiotic processes.[6,8,9]

The reductive dissolution of Fe(III) (oxyhydr)oxides can proceed by both biotic and abiotic means via dissimilatory Fe(III)-reducing bacteria (e.g., *Shewanella* or *Geobacter* species) or geochemical reduced species, such as reduced HA and sulfide. Bioreduction of Fe(III) and humic substances was recently suggested to play a major role in anaerobic respiration in Arctic peat soils.[10] Dissimilatory iron reduction (DIR) of Fh may result in the formation of secondary Fe minerals, such as goethite,[11] magnetite,[12,13] GR,[14] vivianite,[15,16] or siderite.[17] Considering the ecological and environmental importance of DIR, an extensive amount of research has been conducted over the past decades with various pure synthetic Fe(III) (oxyhydr)-oxides as electron acceptors. In nature, other cations, such as Al^{3+}, Si^{4+}, or OM are often incorporated in Fe(III) (oxyhydr)-oxides.[3,18,19] For example, Fh is a poorly crystalline Fe oxyhydroxide that is ubiquitous in soils and aquatic environments[1,3] and often found associated with OM.[20−22] In a Colorado stream where lead and zinc mining is operated near the headwaters, dissolved OM and Fe/Al ions form coprecipitates, containing up to 10% of organic carbon.[23] In addition, the sorptive stabilization of OM by Fe(III) (oxyhydr)oxides has also been proposed to protect OM from microbial degradation and plays a major role in carbon

Received: June 25, 2013
Revised: November 8, 2013
Accepted: November 12, 2013
Published: November 12, 2013

sequestration.[24−26] Lalonde et al. proposed that 21.5% of the OM in sediments is bound to Fe through coprecipitation (resulting in an average C/Fe molar ratio of 4.0 ± 2.8) and direct chelation resulting in an important OM preservation pathway. [27]

In contrast to the studies of Fe's role in OM stabilization,[5] only a limited number of studies have investigated the impact of OM associated with Fe(III) minerals on biogeochemical iron cycling processes, such as reductive dissolution and secondary mineral formation. The associations of 2-line Fh or goethite with cellular-derived organic compounds have been shown to form under anoxic conditions by Fe(II)-oxidizing bacteria. The characterization of these particles revealed an intimate association of the Fe minerals with the organic molecules and a lower surface area compared to abiotically synthesized, pure Fe(III) minerals.[28,29] Fh synthesized abiotically in the presence of polysaccharides via hydrolysis was also found to have lower specific surface area compared to pure Fh due to stronger aggregation of the coprecipitated particles.[30] Organic matter or organic acids can also stabilize Fh, thus preventing the transformation to more crystalline goethite or hematite.[31,32] For example, natural Fh containing OM was aged under conditions favorable for goethite formation (boiled in a strong alkaline solution). The natural Fh remained as Fh, while pure lab synthesized Fh transformed to goethite.[31] Given the fact that OM coprecipitation can alter the physical and chemical properties of Fh and ultimately the fate and transport of OM, Fe, nutrients, and contaminants, it is important to understand how OM coprecipitation affects microbial Fe(III) mineral reduction, dissolution, and secondary mineral formation. To our knowledge, there are no studies exploring the effect of OM coprecipitation on the bacterial reduction and transformation of Fh. In a recent study, Al substituted Fh was reduced significantly slower than pure Fh by *Shewanella putrefaciens* CN32.[18] A second recent study showed that microbially derived biomass that was coprecipitated with Fe(III) oxyhydroxides by Fe(II)-oxidizing bacteria significantly influenced As mobility during reduction of As-loaded biogenic Fe(III) minerals.[33] Yet, it is uncertain if OM coprecipitation would have similar effects on the Fe(III) reduction rate.

Thus, the main objectives of this research are to investigate the impact of coprecipitated HA on DIR and on the secondary mineralization of Fh in order to improve our current understanding of the bioavailability and reactivity of Fe (oxyhydr)oxides present in various environments.

MATERIALS AND METHODS

A detailed Methods description is provided in the Supporting Information (SI).

Materials. All compounds used here are reagent grade, and 18 MΩ doubly deionized water was used to prepare stock solutions. Humic acid was purchased from the International Humic Substance Society (Atlanta, GA) as Elliot Soil Humic Acid Standard. *Shewanella putrefaciens* strain CN32 was obtained from the American Type Culture Collection (ATCC, Manassas, VA).

Coprecipitate Synthesis. Two-line Fh was prepared by neutralization of a 50 mM $FeCl_3 \bullet 6H_2O$ solution (initial pH of 2.1) with 0.4 M NaOH to a pH of 7.5 followed by repeated (5 times) washing/centrifugation (1753 g) steps with deionized water to remove excess ions. Ferrihydrite humic acid (Fh-HA) coprecipitates were synthesized by mixing a $FeCl_3 \cdot 6H_2O$ solution (pH 2.1) with a HA solution at various C/Fe ratios and then raising the pH up to 7.5 by the addition of NaOH. Throughout the manuscript, Fh-HA coprecipitates are referred to as C/Fe molar ratios of C/Fe = 0.4, 0.8, 1.8, and 4.3. Ferrihydrite and Fh-HA coprecipitates were coated on quartz sand as described previously.[34]

Analytical Procedures. The mineralogy of Fh and the Fh-HA coprecipitates were characterized using dry powder X-ray diffraction (XRD). In addition, the electrophoretic mobility (EM) was measured to study the surface charge of the particles, using a ZetaPals Zeta Potential Analyzer (Brookhaven Instrument Corp., Brookhaven, NY). Brunauer−Emmett−Teller (BET) surface area analysis was performed, using an ASAP2020 Physisorption Analyzer (Micromeritics Instrument Corp., Norcross, GA). Scanning transmission X-ray microscopy (STXM) images were collected at beamline 5.3.2.2 and 11.0.2 at the Advanced Light Source, Berkeley, CA and at SM beamline 10ID-1 at the Canadian Light Source, Saskatoon, Canada. Coprecipitates were suspended in DDI water, and a droplet was deposited on a TEM grid for the analysis. Data were collected at C 1s and Fe 2p edges and processed, using the program aXis 2000.[35]

Aqueous and solid phase Fe(II) and total Fe (after digestion in 6 M trace metal grade HCl for 24 h under oxic condition) were determined spectrophotometrically using the Ferrozine method.[36] Samples for X-ray absorption spectroscopy (XAS) analyses were sonicated (<4 h) to remove the coprecipitates from the sand, and then wet pastes were sealed between two pieces of Kapton tapes. The local structural environment of Fe was determined using the extended X-ray absorption fine structure (EXAFS) region of XAS at the Stanford Synchrotron Radiation Laboratory (SSRL) on beamline 11−2 and 4−1, running under dedicated conditions. The XAS analytical procedure used here were similar to those described previously.[11,37,38] A set of Fe reference compounds was used to perform linear combination fitting (LCF) on k^3-weightened EXAFS spectra using the SIXPACK interface to IFEFFIT.[39] Reference compounds were chosen based on their likelihood of being a reaction product (including, for example, criteria such as elemental composition), and were included in the fit only if they contributed with a fraction of 5% or more. Detection limit for minor constituents is approximately 5%.[37]

^{57}Fe−Mössbauer spectroscopy was used to identify Fe mineral phases after 12 days of inoculation with CN32 to help constrain the EXAFS LCF procedure. In general, mineral phases containing as little as 2% of total Fe can be identified with this technique. The coprecipitate coated sand was sonicated (10 min) to remove the coprecipitate from the sand particles. Suspensions of the coprecipitate were shipped in an anoxic container to Tübingen and stored in an anoxic glovebox until Mössbauer analysis. Coprecipitate samples were sealed between two pieces of Kapton tapes in an anoxic glovebox. Mössbauer spectra were obtained with a standard transmission setup (Wissel) using a triangular velocity waveform and a ^{57}Co source in rhodium matrix. The Mössbauer data were modeled with the Recoil software (University of Ottawa, Canada) using its Voigt-based fitting analysis routine (see SI for a detailed description).

Experimental Setup. The role of coprecipitated HA on microbial Fe(III) reduction and secondary mineralization pathways was investigated by inoculation of the Fh or Fh-HA coprecipitate coated sand for 12 days with *S. putrefaciens* CN32 to a cell density of ~10^8 mL^{-1}. The preparation of bacterial cultures was described previously.[11] Synthetic groundwater

medium (SGM) at pH 7.2 was used in all experiments, and sodium lactate (3 mM) was added as an electron donor.[11] All experiments were prepared in an anoxic glovebag (Coy Laboratories, Inc., Grass Lake, MI), containing an anoxic gas mixture (N_2 95%; H_2 5%). Reactions were performed in 125 mL serum bottles containing SGM purged with O_2-free N_2 gas, microbes, and 5 g of coprecipitates. The bottles were crimp sealed with butyl rubber septa. Each treatment was replicated three times. Sterilized (autoclaved 15 min at 121 °C) control setups consisted of anoxic buffer in place of the CN32 cell suspension. Triplicate samples were placed on a horizontal shaker at 80 rpm at 22 °C and sampled periodically for analyses. No Fe reduction was observed in any of the sterilized controls.

The role of dissolved HA on the microbial reduction of coprecipitates was also investigated. Similar to the experiments described above, coprecipitates (C/Fe = 0.4) were inoculated with CN32 in SGM but in the concurrent presence of initial (before sorption) dissolved HA concentrations of 2 mg HA/L, 10 mg HA/L, and 50 mg HA/L.

RESULTS

Characteristics of Coprecipitates. The effect of coprecipitated HA on the crystal structure of Fh-HA coprecipitates was investigated using XRD. Regardless of the C/Fe ratio, the XRD patterns for all coprecipitates showed two broad peaks, resembling 2-line Fh (SI Figure S1). The EM and point of zero charge (PZC) were significantly lower for the coprecipitates than for pure Fh particles (SI Figure S9). The PZC for pure Fh was approximately at pH 8.25. For the C/Fe = 0.4 coprecipitates, PZC dropped to approximately pH 5.25, and the C/Fe = 0.8, 1.8, and 4.3 coprecipitates were all negatively charged in the pH range from 5 to 9.5. The specific surface area (SSA) analysis showed decreasing SSA as a function of increasing C/Fe ratios (Table 1). The SSA of Fh (before coating on sand) was determined to be 240 m^2/g, whereas the SSA dropped to 180 m^2/g for C/Fe=0.4 and to 70 m^2/g for C/Fe = 4.3. In addition, the spatial distribution of HA within coprecipitates was investigated, using STXM. STXM analysis of the C/Fe = 0.4 coprecipitates indicated that C was distributed rather evenly (Figure 1). Similar STXM observations were made on other coprecipitates (data not shown).

Table 1. C/Fe Ratio, Specific Surface Area (SSA) and Point of Zero Charge (PZC) Determination of Fh-HA Coprecipitates

initial C/Fe ratio (before hydrolysis)	C/Fe ratio of coprecipitates on sand	SSA for Fh-HA coated sand (m^2/g)	SSA for Fh-HA not coated on sand (m^2/g)	PZC for Fh-HA coprecipitates not coated on sand (pH)
C/Fe = 0	0	4 ± 0.27	240	≈ 8.25
C/Fe = 0.5	0.4	2.5 ± 0.46	180	≈ 5.25
C/Fe = 1.5	0.8	0.42 ± 0.16	100	<5
C/Fe = 2.5	1.8	0.25 ± 0.006	80	<5
C/Fe = 6	4.3	0.20 ± 0.015	70	<5

Effect of HA on the Rate and Extent of Dissimilatory Fe(III) Reduction. The effect of coprecipitated HA on dissimilatory Fe(III) reduction was investigated by incubating the coprecipitates with *S. putrefaciens* CN32 under anoxic conditions. The Fh-HA coprecipitates were coated on quartz sands to better represent natural environments where Fe(III) (oxyhydr)oxides often exist as coatings on soil particles.[3] Over the course of 12 days, Fe(III) was continuously reduced to Fe(II) in all samples (Figure 2), and the rate of Fe(III) reduction was found to vary as a function of the C/Fe ratio. The highest Fe(III) reduction rate was observed for the coprecipitates containing the highest fraction of C (C/Fe = 4.3), whereas the lowest Fe(III) reduction rate was observed for the coprecipitates with low C fraction of C/Fe = 0.4 and 0.8. The Fe(III) reduction rate for pure Fh (C/Fe = 0) and C/Fe = 1.8 coprecipitates fell in the middle. Increasing C/Fe ratio in the coprecipitates resulted in a concurrent increase of solid phase associated Fe(II) (Figure 2). The data from Figure 2 are replotted to also allow for a comparison of the relative distribution of Fe(II) in the aqueous phase and solid phase (SI Figure S3). In general, the relative concentration of Fe(II) in the aqueous phase increases, and Fe(II) in the solid phase decreases over time. During the course of the 12 day incubation, any measurable amount of HA was not released into the aqueous phase.

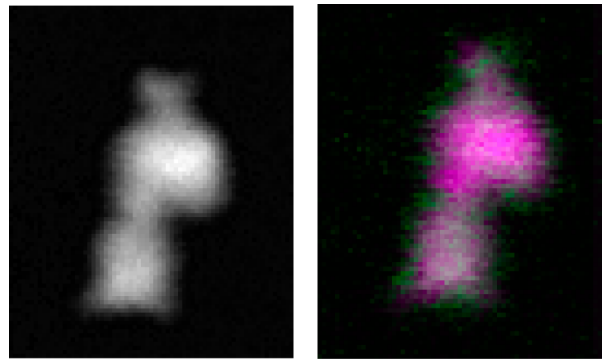

Figure 1. STXM analysis of C/Fe = 0.4 Fh-HA coprecipitates. The left image is an optical density representation of the Fe-distribution. The right image is showing the distribution of carbon (in green) and iron (in pink). Each image is 1.7 × 2 μm.

In addition to investigating the sole effect of coprecipitated HA, the combined effect of dissolved HA and coprecipitated HA on ferrihydrite reduction was investigated by the addition of HA to setups, containing C/Fe = 0.4 coprecipitates and *S. putrefaciens* CN-32 (Figure 3). Sorption isotherm studies with C/Fe = 0.4 coprecipitates were conducted to determine the amount of sorbed HA. The results indicated that a significant portion of the added HA was adsorbed to the coprecipitates, resulting in aqueous HA concentrations of 0.4, 3.2, and 35.9 mg/L for systems with initially added 2, 10, and 50 mg/L of HA, respectively (SI Figure S5). The addition of 2 and 10 mg HA/L resulted in slightly lower Fe(III) reduction rates, whereas addition of 50 mg HA/L resulted in similar or greater Fe(III) reduction rates than systems not added dissolved HA (Figure 3).

Role of Coprecipitated HA on Secondary Mineralization Pathways of Fh-HA. Secondary Fe mineral phases formed during microbial reduction were determined using EXAFS LCF analysis and Mössbauer spectroscopy. Based on EXAFS LCF analysis, in the pure Fh (C/Fe = 0) setup, 41% of the Fh was transformed to goethite (17%), magnetite (18%), and GR (6%) (Table 2), and the remaining 59% maintained Fh structure. The ~5 K Mössbauer spectrum of this system confirms the transformation to goethite (SI Figure S6, SI Table S1). Magnetite was not observed in this spectrum but ferrous GR was observed in the 77 K spectrum (Figure 4). Kukkadapu

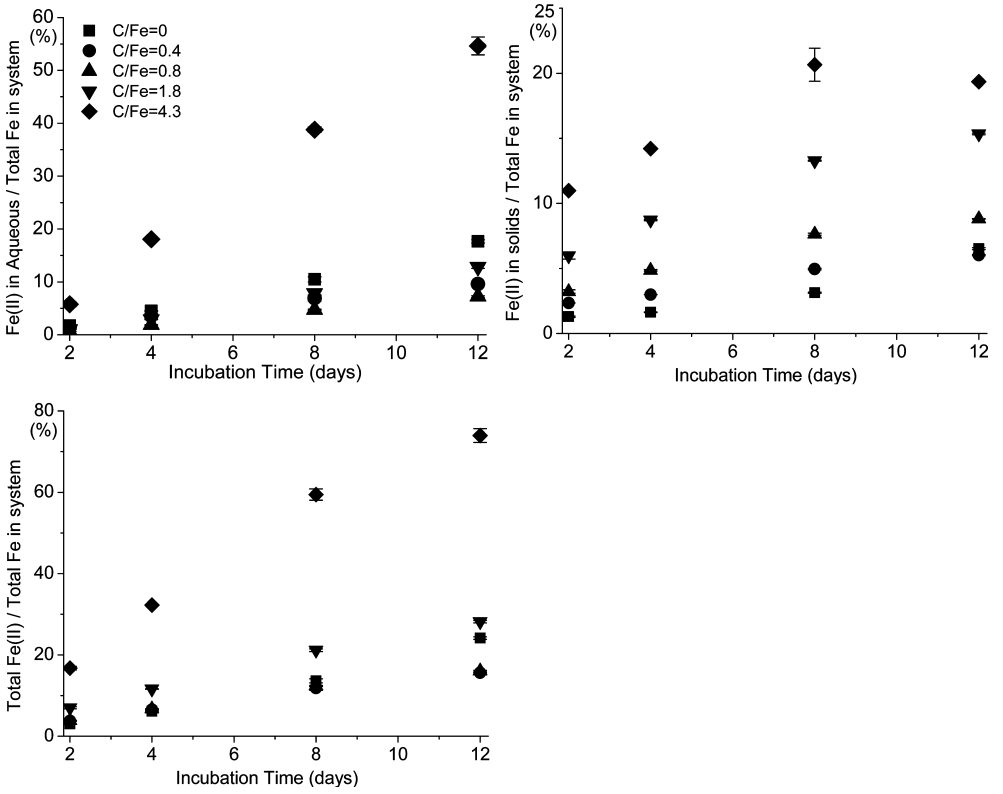

Figure 2. Fe(II) production in Fh-HA coprecipitate setups inoculated with Fe(III)-reducing bacteria (*Shewanella putrefaciens* strain CN-32). The amount of Fe(III) reduction is normalized to the initial amount of Fe in the coprecipitates.

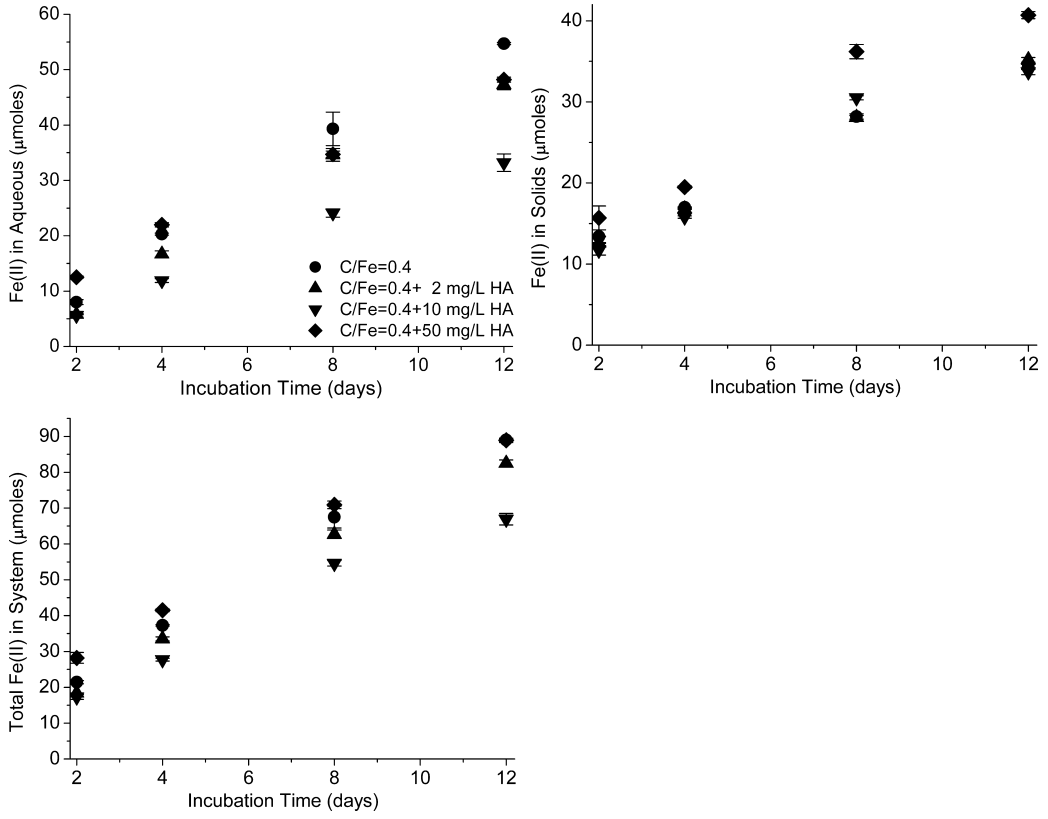

Figure 3. Effect of dissolved HA on Fe(II) production in systems with *Shewanella putrefaciens* CN-32 and coprecipitates with a molar C/Fe ratio of 0.4. The Fh-HA coprecipitate coated sand and CN-32 was incubated for 12 days under the same condition as experiments shown in Figure 2

Table 2. *Shewanella putrefaciens* Strain CN32 Induced Conversion of Ferrihydrite-Humic Acid (Fh-HA) Coprecipitates As a Function of C/Fe Ratio Following 12 Days of Incubation[a]

	Fh-HA coprecipitate (%)	goethite (%)	[b]magnetite (%)	green rust (%)	reduced chi^2
C/Fe = 0	59	17	18	6	0.060
C/Fe = 0.4	85	0	9	6	0.036
C/Fe = 0.8	82	0	8	10	0.039
C/Fe = 1.8	74	0	10	16	0.052
C/Fe = 4.3	60	0	10	30	0.073

[a]The secondary Fe mineral phases formed are presented as mole% Fe. [b]Note that magnetite was not observed by Mössbauer spectroscopy. For EXAFS fit without inclusion of magnetite see Table S3.

et al.[40] reported long-term instability of magnetite that had formed upon DIR using the same bacterial strain (CN32) as we did. They observed ferrous hydroxy carbonate as the transformation product of magnetite. However, the Mössbauer parameters they reported for that mineral are not consistent with our data. EXAFS analysis showed that upon Fh coprecipitation with HA, the extent of Fh transformation drops from 41 to 16% at C/Fe = 0.4, clearly showing that the coprecipitated HA limits the secondary mineralization of Fh. A similar decrease (to 22%) was observed for C/Fe = 1.8. However, the extent of transformation has a parabolic trend in that a similar extent of original material was transformed for pure Fh and the coprecipitates with the highest C fraction (C/Fe = 4.3).

In addition, the secondary Fh mineralization pathways were also altered by the HA coprecipitation. Coprecipitated HA inhibited the formation of a secondary goethite phase (Table 2). While goethite represents 17% of the secondary Fe phases in pure Fh systems, goethite was not present or below the EXAFS detection limit (ca. 5%) in all systems containing coprecipitates. Mössbauer analysis confirmed the absence of goethite (SI Table S1). Also, the amount of secondary magnetite was reduced by the HA coprecipitation from approximately 20% in C/Fe = 0 to approximately 10% for all coprecipitates based on EXAFS LCF analysis. While the HA coprecipitation inhibited the formation of goethite and magnetite, the coprecipitation stimulated the formation of a green rust-like phase. Based on EXAFS LCF analysis, approximately 30% of the coprecipitates were transformed to GR in the C/Fe=4.3 systems. While magnetite was not observed in the Mössbauer spectra of the C/Fe 0.4 and 1.8 systems, a ferrous green rust-like phase appeared in the spectra and increased with increasing C/Fe ratio (SI Figure S6, SI Table S1). The C/Fe = 4.3 system was not analyzed with Mössbauer spectroscopy.

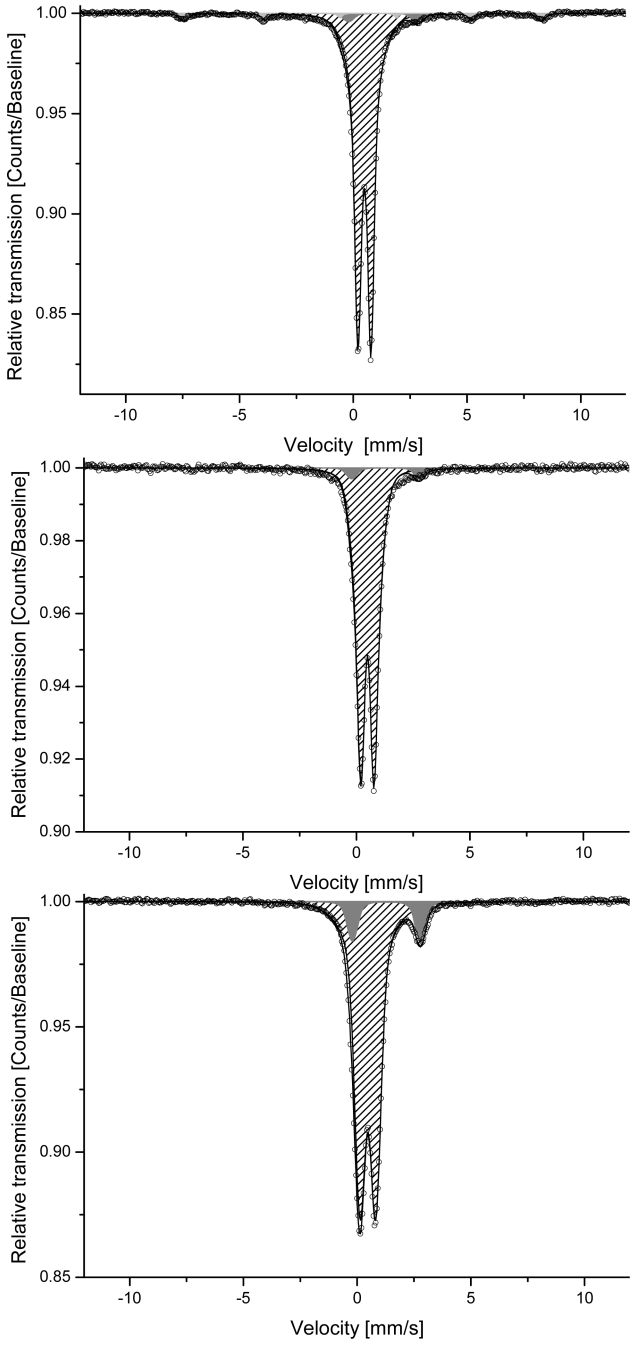

Figure 4. Mössbauer spectra obtained at 77 K of coprecipitates following 12 days incubation with *Shewanella putrefaciens* CN-32. Top: C/Fe = 0; middle: C/Fe = 0.4; bottom: C/Fe = 1.8. Hatched doublet: Ferrihydrite; light-gray sextet: goethite; gray doublet: Ferrous green rust.

DISCUSSION

Effect of HA on Fh-HA Coprecipitate Reduction. The results consistently indicate that coprecipitation with a low C/Fe ratio or the presence of a small amount of additional dissolved HA or adsorbed HA decreases the Fe(III) reduction rates, while higher C/Fe ratios or the presence of a high concentration of additional dissolved HA enhances the Fe(III) reduction rates (Figures 2 and 3). Possible explanations for these observations may be related to the role of HA as an electron shuttle,[41] a strong ligand,[19] or in particle aggregation.[42]

It has been established that humic substances can enhance Fe(III) reduction rates via an electron shuttling mechanism.[43] Previous studies report that in order to enhance the Fh reduction rate via HA electron shuttling, a threshold amount of dissolved C (at least 5−10 mg dissolved C/L) has to be present in the solution.[44] In addition, solid-phase humic substances are capable of shuttling electrons as well, transferring electrons from microbes to Fe(III) oxides.[41] These results imply that coprecipitated HA also may transfer electrons and require a threshold amount of C to enhance the Fe(III) reduction rate via electron shuttling in the system. For the C/Fe = 0.4 and 0.8

coprecipitates, the amount of C may not be sufficient to support electron shuttling. However, high fractions of C (C/Fe = 1.8 and C/Fe = 4.3) may stimulate electron shuttling, which may explain the higher observed reduction rates (Figure 2). In setups containing C/Fe = 0.4 coprecipitates with 2 and 10 mg/L dissolved HA addition, less than 5 mg/L of dissolved C is present in the solution (SI Figure S5), which could indicate that the dissolved HA was not sufficient to enhance Fe(III) reduction via electron shuttling. For the setup with additional 50 mg/L HA, approximately 36 mg/L of HA is present in solution as dissolved HA, which is equivalent to 20 mg C/L. The amount of dissolved HA in this setup is, in theory, sufficient to enhance the Fe(III) reduction (>5 mg C/L threshold).[44] Enhanced Fe(III) reduction rates are observed at day 2, 4, and 8 compared to setups without HA addition, but the electron shuttling effect diminishes by day 12. This could be due to the formation of more crystalline Fe(II) containing minerals, such as magnetite or GR (described in detail below), which may result in surface passivation by sorbed or structural Fe(II), or changes in the mineral redox potential. An alternative explanation could be the presence of microbially produced flavines by *S. putrefaciens* with electron shuttling capacity[45,46] which potentially could outcompete HA as an electron shuttle.

HA is likely to impact the reactivity or reducibility of Fh in multiple ways depending on its concentration and mode of sorption (e.g., adsorption vs coprecipitation). Previous research indicates that Fe(III) forms stable mononuclear complexes with natural organic matter (NOM) via carboxylic and hydroxyl functional groups.[47−49] Thus, hydrolysis of Fe(III) in the presence of HA may first result in mononuclear Fe-HA complexation at low pH followed by coprecipitation of Fh and HA at higher pH. The amount of coprecipitated or physically bound HA versus chemically complexed HA would then depend on the amount of potential reactive Fe(III) sites or the HA concentration. It has been proposed that mononuclear complexation of NOM to Fe(III) limits hydrolysis and precipitation of Fe(III) and may also impact the properties of the Fh formed.[48] The Mössbauer analysis further supports this hypothesis since the mean magnetic hyperfine field for the initial coprecipitates is lower compared to pure Fh.[30,50] The decrease in mean magnetic hyperfine field has been proposed to be related to a decrease in the interparticle interactions of individual Fh particles,[50,51] which implies that the adsorbed or coprecipitated HA is reducing the amount of potential reactive surface sites. The blockage of Fe surface sites by HA might not only suppress the electron transfer but also contribute to the repulsion of bacteria from the coprecipitate due to the influence of HA on the zeta-potential of the coprecipitate.[42] The EM studies showed that the HA coprecipitation resulted in more negatively charged particles above pH 5 (SI Figure S9). *S. putrefaciens* CN32 cells are also negatively charged due to their lipopolysaccharide layers which may result in decreased cell-mineral interactions and electron transfer.[52] However, it is noted that we measured the EM of the coprecipitates before they were coated on silica sand for analytical reasons. Since silica sands have a PZC around pH 2, it is difficult to determine if there were any significant difference in electrostatic repulsion between the cells and the different types of Fh used in these experiments.[53]

In addition, the coprecipitated HA resulted in a large decrease in specific surface area (SSA) with increasing C/Fe ratio for both uncoated coprecipitates and coprecipitates coated on sands (Table 1). It has been reported that microbial Fe(III) reduction is proportional to the SSA of Fe (oxyhydr)oxide minerals, regardless of the degree of crystallinity or crystal structures.[54] Thus, it is likely that the smaller SSA may have limited the reduction of the low C/Fe ratio coprecipitates (C/Fe = 0.4 and 0.8). The decrease in the SSA of coprecipitates is likely due to multiple factors such as formation of larger aggregates promoted by the coprecipitated HA, lower Fh content or blocking of Fh sites by HA.[30,50] It may be assumed that the aggregation took place during the initial coprecipitate synthesis, because the coprecipitates coated on sands also show a similar SSA decrease as a function of increasing C/Fe ratio. Coating of Fe-oxides onto sand limits further aggregation during the incubation period due to decreased interactions among Fe oxide particles. Thus, aggregation effects as observed in systems with suspended Fe-oxides are not expected to the same degree due to surface-promoted stabilization via binding to the silica sand.[42] Drying and coating as well as reaction with Si and Al have also been reported to impact Fh reactivity.[55,56]

The Fe(III) reduction rates for coprecipitates with a C/Fe ratio of 0.4 and 0.8 may be suppressed because the effect of surface site blocking or aggregation is greater than electron shuttling by HA, while electron shuttling or increased Fh reduction becomes more relevant at higher C/Fe ratios (1.8 and 4.3). In addition, it is possible that a significant fraction of occluded HA rather than adsorbed HA must be present for electron shuttling to occur within the Fh particles.[57]

Secondary Mineralization Pathways of Fh-HA Coprecipitates. In addition to the extent of transformation being modified, the transformation pathway was also modified by the HA coprecipitation. Previous studies have shown that the transformation products formed via dissimilatory Fh reduction (e.g., goethite, magnetite, siderite, GR) are controlled by factors such as pH,[58] buffer system,[59] Fe(III) reduction rate,[60] cell concentration,[61] Fe(II) concentration,[62] isomorphic substitution,[55] adsorbed ions,[11] and particle aggregation.[42]

In this study, the most notable difference in the secondary Fe phases formed in the presence of HA is the apparent inhibition of goethite precipitation and formation of a green rust-like phase. Previous studies reported that adsorbed species, such as phosphate or Pahokee Peat Humic Acid, can inhibit goethite formation during the reduction of Fh by *S. oneidensis* strain MR-1 or Fh coated sand by *S. putrefaciens* strain CN-32.[11,63] In the presence of Fh, goethite can be formed by aggregation based crystal growth or the dissolution and recrystallization of Fh.[3,64] The dissolution and recrystallization pathway is also likely affected by coprecipitated HA. Aqueous Fe(II) produced via reductive dissolution can adsorb to Fh and catalyze the transformation of Fh to goethite.[65] In this study, no goethite was formed in systems containing HA irrespective of whether low or high concentrations of dissolved Fe(II) were produced. Thus, coprecipitated HA likely blocked reactive Fh surface sites, limiting the amount of Fe(II) directly adsorbed on the Fh surface, and therefore inhibiting the Fe(II) catalyzed goethite formation through dissolution and recrystallization pathways.[42,60]

Another effect of coprecipitated HA on the secondary Fe mineral phases is the reduction of magnetite formation, which agrees with previous work showing that the presence of phosphate or HA can inhibit magnetite formation.[11,42,63,66] It has been proposed that magnetite can form in Fh containing systems by nucleation and crystallization or solid state reduction and transformation.[62,67,68] Solid state transformation has been proposed to be the major pathway in systems with

high electric current density or Fe(II) concentration (≥1.8 mM).[68] At low electric current density or low Fe(II) concentration (≤1.8 mM Fe(II)), magnetite is formed via nucleation and crystallization, whereby the exact mechanism of magnetite formation remains uncertain.[68] However, it has been proposed that at low electric current density or low Fe(II) concentration, both goethite and magnetite can form simultaneously. The only system that resulted in Fe(II) concentrations close to 1.8 mM was the one containing pure Fh (i.e., 1.6 mM $Fe(II)_{total}$ or 1.2 mM $Fe(II)_{aq}$), which supports the higher observed magnetite formation (18% of initial Fh). All other Fh-HA coprecipitate setups contained between 0.3 (C/Fe = 0.8) and 0.7 (C/Fe = 4.3) mM $Fe(II)_{aq}$ resulting in a 50% reduction of the magnetite formed relative to the HA free systems based on LCF EXAFS analysis. Despite the apparent inhibition of goethite formation by coprecipitated HA, it did not enhance the formation of magnetite through a nucleation and crystallization pathway.[68] Thus, the inhibition of magnetite formation is likely a result of a low Fe(II) concentration, blocking of surface sites, or HA induced aggregation.

In contrast to goethite and magnetite, the formation of a green rust-like phase was stimulated by coprecipitated HA based on EXAFS and Mössbauer analysis (SI Figure S6). GR minerals are mixed-valence layered Fe(II)/Fe(III) hydroxide plates with common interlayer anions such as chloride, sulfate, and carbonate. In this study, GR carbonate is the most likely product, based on EXAFS and Mössbauer spectroscopy analysis and low sulfate concentration in the SGM (≈200 μM).[69] Unlike the effect of coprecipitated HA on dissimilatory Fe(III) reduction kinetics, the amount of GR formation is proportional to the C/Fe ratio or increasing aggregation of the Fh-HA, which may be an indication that the coprecipitated HA is stimulating the GR formation. It was recently reported that "a high bacterial cell to lepidocrocite ratio leads to densely packed aggregates and GR formation while at lower cell densities looser aggregates were formed and magnetite was systematically produced."[70] The aggregate structure created by the presence of a biofilm has been proposed to result in microenvironments that may favor locally high concentrations of bicarbonate and Fe(II) due to diffusion limitations ultimately resulting in ferrous bearing phases such as GR.[70−73] A similar hypothesis that may apply in this study is that coprecipitated HA entraps Fe(II) and bicarbonate, thereby concentrating these species within diffusion limited microenvironments resulting in (ferrous) green rust (Table 2 and SI Table S2).

There were some discrepancies in the Fe phases determined by EXAFS and Mössbauer analysis. The most significant difference was that the presence of magnetite was only suggested by LCF EXAFS analysis with 18% magnetite produced in systems containing pure ferrihydrite and approximately 10% in systems containing Fh-HA coprecipitates. Similar findings were observed in studies on the effect of phosphate on the mineralization pathway of ferrihydrite.[11] However, mössbauer analysis showed no evidence of magnetite. One possible explanation is that the formed magnetite was nanoparticulate, that is, superparamagnetic. In that case, it would not be resolvable from the ferrihydrite doublet observed at temperatures of 77 K and above. Below the Verwey transition, magnetite spectra become complicated with up to five sextets. The amounts of magnetite indicated by EXAFS may be difficult to resolve from the ferrihydrite sextets.[74] In addition, the magnetite reference spectra used for LCF EXAFS analysis may not perfectly represent the magnetite produced in our systems due to different crystallinity possibly resulting in an overestimation of the actual amount. We attempted LCF EXAFS analysis without inclusion of the magnetite reference spectra (SI Table S3). The reduced chi square value almost doubled for the system containing pure ferrihydrite (C/Fe = 0), which implies that magnetite is likely present. The reduced chi square values did not change dramatically in systems containing Fh-HA coprecipitates. One possible explanation is that Fe adsorbed to HA or bacteria and Fe phases not included in the LCF EXAFS analysis may have resulted in spectral features that were better fitted with inclusion of magnetite (for further discussion see SI).

Environmental Significance. The coprecipitation of organic matter (OM) with Fe (oxyhydr)oxide minerals is a commonly observed phenomenon in the environment.[22] Previous studies have also shown that in contrast to pure Fh, Fh-OM coprecipitates are more stable and do not easily transform into more crystalline phases such as goethite and hematite even after long-term aging under high temperature.[31,32,48,75,76] These observations along with observations from this study may help to explain why soils and sediments often contain substantial amounts of Fh-like phases.[31] Also, this study demonstrates that coprecipitated HA influences the fate and reactivity of Fh under dissimilatory Fe(III) reduction conditions. These observations could have implications for predicting the impact of OM on biological Fe reduction in climate sensitive areas such as Arctic peat soils where biological Fe and OM reduction has been proposed to play an important role in anaerobic respiration which may influence terrestrial CO_2 and CH_4 fluxes.[10] In addition, the observed changes in the secondary Fe mineralization pathway for the Fh-HA coprecipitates relative to pure Fh are likely to influence many environmentally relevant factors, such as mobility, bioavailability, and redox reactivity of Fe minerals. GR can for instance easily reduce U(VI) to U(IV), forming nanoscale UO_2 compounds.[77,78] However, it is largely unknown if GR formed in the presence of OM is as reactive as pure GR. In summary, this study suggests that the quantities of coprecipitated, adsorbed, and dissolved OM should be considered when evaluating the biological reactivity and transformation of Fe (oxyhydr)oxide minerals in the environment.

■ ASSOCIATED CONTENT

Ⓢ Supporting Information

A more detailed method section, additional figures and tables, coprecipitate XRD patterns, Fe EXAFS spectra, SEM images, distributions and concentrations of Fe(II) and Fe(III) in various systems, and Mössbauer spectra, parameters and interpretation, are provided. This Material is available free of charge via the Internet at http://pubs.acs.org.

■ AUTHOR INFORMATION

Corresponding Author

*(T.B.) Phone: +1-970-491-6235; fax: +1-970-491-0564; e-mail: thomas.borch@colostate.edu.

Notes

The authors declare no competing financial interest.

■ ACKNOWLEDGMENTS

This work was funded by a National Science Foundation CAREER Award (EAR0847683). This project was partly supported by Agriculture and Food Research Initiative

Competitive Grant no. 2013-67019-21359 from the USDA National Institute of Food and Agriculture. We acknowledge technical support from beam line scientists at SSRL, ALS, and CLS to obtain data. We also appreciate comments from Dr. Ravi Kukkadapu on an earlier version of the manuscript. Portions of this research were carried out at the Stanford Synchrotron Radiation Lightsource, a Directorate of SLAC National Accelerator Laboratory and an Office of Science User Facility operated for the U.S. Department of Energy Office of Science by Stanford University. Portions of the research described in this paper were performed at the Canadian Light Source, which is supported by the Natural Sciences and Engineering Research Council of Canada, the National Research Council Canada, the Canadian Institutes of Health Research, the Province of Saskatchewan, Western Economic Diversification, and the University of Saskatchewan. Portions of research described in this paper were performed at the Advanced Light Source. The Advanced Light Source is supported by the Director, Office of Science, Office of Basic Energy Sciences, of the U.S. Department of Energy under Contract No. DE-AC02-05CH11231. A.K. thanks the German Research Foundation (KA1736/3-2; research group FOR 580 "Electron Transfer Processes in Anoxic Aquifers") for funding. Martin Obst was supported by the Emmy-Noether Program of the DFG (OB 362/1-1). Christian Schroder acknowledges funding through the DFG research group FOR 580.

REFERENCES

(1) Jambor, J. L.; Dutrizac, J. E. Occurrence and constitution of natural and synthetic ferrihydrite, a widespread iron oxyhydroxide. *Chem. Rev.* **1998**, *98* (7), 2549−2585.

(2) Schwertmann, U. Solubility and dissolution of iron-oxides. *Plant Soil* **1991**, *130* (1−2), 1−25.

(3) Cornell, R. M.; Schwertmann, U., *The Iron Oxides: Structure, Properties, Reactions, Occurences, and Uses*; Wiley-VCH, 2003.

(4) Hochella, M. F.; Lower, S. K.; Maurice, P. A.; Penn, R. L.; Sahai, N.; Sparks, D. L.; Twining, B. S. Nanominerals, mineral nanoparticles, and earth systems. *Science* **2008**, *319* (5870), 1631−1635.

(5) Kaiser, K.; Guggenberger, G. Sorptive stabilization of organic matter by microporous goethite: Sorption into small pores vs. surface complexation. *Eur. J. Soil Sci.* **2007**, *58* (1), 45−59.

(6) Borch, T.; Kretzschmar, R.; Kappler, A.; Van Cappellen, P.; Ginder-Vogel, M.; Voegelin, A.; Campbell, K. Biogeochemical redox processes and their impact on contaminant dynamics. *Environ. Sci. Technol.* **2010**, *44* (1), 15−23.

(7) Shimizu, M.; Arai, Y.; Sparks, D. L. Multiscale assessment of methylarsenic reactivity in soil. 2. Distribution and speciation in soil. *Environ. Sci. Technol.* **2011**, *45* (10), 4300−4306.

(8) Konhauser, K. O.; Kappler, A.; Roden, E. E. Iron in microbial metabolisms. *Elements* **2011**, *7* (2), 89−93.

(9) Pantke, C.; Obst, M.; Benzerara, K.; Morin, G.; Ona-Nguema, G.; Dippon, U.; Kappler, A. Green rust formation during Fe(II) oxidation by the nitrate-reducing Acidovorax sp strain BoFeN1. *Environ. Sci. Technol.* **2012**, *46* (3), 1439−1446.

(10) Lipson, D. A.; Jha, M.; Raab, T. K.; Oechel, W. C. Reduction of iron (III) and humic substances plays a major role in anaerobic respiration in an Arctic peat soil. *J. Geophys. Res.: Biogeosci.* **2010**, 115.

(11) Borch, T.; Masue, Y.; Kukkadapu, R. K.; Fendorf, S. Phosphate imposed limitations on biological reduction and alteration of ferrihydrite. *Environ. Sci. Technol.* **2007**, *41* (1), 166−172.

(12) Heron, G.; Christensen, T. H.; Tjell, J. C. Oxidation capacity of aquifer sediments. *Environ. Sci. Technol.* **1994**, *28* (1), 153−158.

(13) Lovley, D. R.; Stolz, J. F.; Nord, G. L.; Phillips, E. J. P. Anaerobic production of magnetite by a dissimilatory iron-reducing microorganism. *Nature* **1987**, *330* (6145), 252−254.

(14) Trolard, F.; Genin, J. M. R.; Abdelmoula, M.; Bourrie, G.; Humbert, B.; Herbillon, A. Identification of a green rust mineral in a reductomorphic soil by Mossbauer and Raman spectroscopies. *Geochim. Cosmochim. Acta* **1997**, *61* (5), 1107−1111.

(15) Peretyazhko, T.; Sposito, G. Iron(III) reduction and phosphorous solubilization in humid tropical forest soils. *Geochim. Cosmochim. Acta* **2005**, *69* (14), 3643−3652.

(16) Zachara, J. M.; Fredrickson, J. K.; Li, S. M.; Kennedy, D. W.; Smith, S. C.; Gassman, P. L. Bacterial reduction of crystalline Fe^{3+} oxides in single phase suspensions and subsurface materials. *Am. Mineral.* **1998**, *83* (11−12), 1426−1443.

(17) Coleman, M. L.; Hedrick, D. B.; Lovley, D. R.; White, D. C.; Pye, K. Reduction of Fe(III) in sediments by sulfate-reducing bacteria. *Nature* **1993**, *361* (6411), 436−438.

(18) Ekstrom, E. B.; Learman, D. R.; Madden, A. S.; Hansel, C. M. Contrasting effects of Al substitution on microbial reduction of Fe(III) (hydr)oxides. *Geochim. Cosmochim. Acta* **2010**, *74* (24), 7086−7099.

(19) Jones, A. M.; Collins, R. N.; Rose, J.; Waite, T. D. The effect of silica and natural organic matter on the Fe(II)-catalysed transformation and reactivity of Fe(III) minerals. *Geochim. Cosmochim. Acta* **2009**, *73* (15), 4409−4422.

(20) Carlson, L.; Schwertmann, U. Natural ferrihydrite in surface deposits from Finland and their association with silica. *Geochim. Cosmochim. Acta* **1981**, *45* (3), 421−429.

(21) Murad, E.; Bowen, L. H.; Long, G. J.; Quin, T. G. Thte influence of crystallinity on magnetic-ordering in natural ferrihydrites. *Clay Miner.* **1988**, *23* (2), 161−173.

(22) Schwertmann, U.; Murad, E. The nature of an iron oxide: Organic iron association in a peaty environment. *Clay Miner.* **1988**, *23* (3), 291−299.

(23) McKnight, D. M.; Wershaw, R. L.; Bencala, K. E.; Zellweger, G. W.; Feder, G. L. Humic substances and trace metals associated with Fe and Al oxides deposited in an acidic mountain stream. *Sci. Total Environ.* **1992**, *118*, 485−498.

(24) Wagai, R.; Mayer, L. M. Sorptive stabilization of organic matter in soils by hydrous iron oxides. *Geochim. Cosmochim. Acta* **2007**, *71* (1), 25−35.

(25) Jones, D. L.; Edwards, A. C. Influence of sorption on the biological utilization of two simple carbon substrates. *Soil Biol. Biochem.* **1998**, *30* (14), 1895−1902.

(26) Kogel-Knabner, I.; Guggenberger, G.; Kleber, M.; Kandeler, E.; Kalbitz, K.; Scheu, S.; Eusterhues, K.; Leinweber, P. Organo-mineral associations in temperate soils: Integrating biology, mineralogy, and organic matter chemistry. *J. Plant Nutr. Soil Sci.* **2008**, *171* (1), 61−82.

(27) Lalonde, K.; Mucci, A.; Ouellet, A.; Gelinas, Y. Preservation of organic matter in sediments promoted by iron. *Nature* **2012**, *483* (7388), 198−200.

(28) Kappler, A.; Schink, B.; Newman, D. K. Fe(III) mineral formation and cell encrustation by the nitrate-dependent Fe(II)-oxidizer strain BoFeN1. *Geobiology* **2005**, *3* (4), 235−245.

(29) Posth, N. R.; Huelin, S.; Konhauser, K. O.; Kappler, A. Size, density and composition of cell-mineral aggregates formed during anoxygenic phototrophic Fe(II) oxidation: Impact on modern and ancient environments. *Geochim. Cosmochim. Acta* **2010**, *74* (12), 3476−3493.

(30) Mikutta, C.; Mikutta, R.; Bonneville, S.; Wagner, F.; Voegelin, A.; Christl, I.; Kretzschmar, R. Synthetic coprecipitates of exopolysaccharides and ferrihydrite. Part I: Characterization. *Geochim. Cosmochim. Acta* **2008**, *72* (4), 1111−1127.

(31) Schwertmann, U. Inhibitory effect of soil organic matter on crystallization of amorphous ferric hydroxide. *Nature* **1966**, *212* (5062), 645−&.

(32) Schwertmann, U. Influence of various simple organic anions on formation of goethite and hematite from amorphous ferric hydroxide. *Geoderma* **1970**, *3* (3), 207−214.

(33) Muehe, M.; Scheer, L.; Daus, B.; Kappler, A. Fate of arsenic during microbial reduction of biogenic vs. abiogenic as-Fe(III)-mineral co-precipitates. *Environ. Sci. Technol.* **2013**, *47* (15), 8297−8307.

(34) Hansel, C. M.; Benner, S. G.; Nico, P.; Fendorf, S. Structural constraints of ferric (hydr)oxides on dissimilatory iron reduction and the fate of Fe(II). *Geochim. Cosmochim. Acta* **2004**, *68* (15), 3217−3229.
(35) Hitchcock, A. P., aXis 2000 written in Interactive Data Language (IDL). 2012. http://uncorn.mcmaster.ca/aXis2000.html.
(36) Stookey, L. L. Ferrozine—A new spectrophotometric reagent for iron. *Anal. Chem.* **1970**, *42* (7), 779−&.
(37) Hansel, C. M.; Benner, S. G.; Neiss, J.; Dohnalkova, A.; Kukkadapu, R. K.; Fendorf, S. Secondary mineralization pathways induced by dissimilatory iron reduction of ferrihydrite under advective flow. *Geochim. Cosmochim. Acta* **2003**, *67* (16), 2977−2992.
(38) Shimizu, M.; Ginder-Vogel, M.; Parikh, S. J.; Sparks, D. L. Molecular scale assessment of methylarsenic sorption on aluminum oxide. *Environ. Sci. Technol.* **2010**, *44* (2), 612−617.
(39) Webb, S. M. SIXpack: A graphical user interface for XAS analysis using IFEFFIT. *Phys. Scr.* **2005**, *T115*, 1011−1014.
(40) Kukkadapu, R. K.; Zachara, J. M.; Fredrickson, J. K.; Kennedy, D. W.; Dohnalkova, A. C.; McCready, D. E. Ferrous hydroxy carbonate is a stable transformation product of biogenic magnetite. *Am. Mineral.* **2005**, *90* (2−3), 510−515.
(41) Roden, E. E.; Kappler, A.; Bauer, I.; Jiang, J.; Paul, A.; Stoesser, R.; Konishi, H.; Xu, H. F. Extracellular electron transfer through microbial reduction of solid-phase humic substances. *Nat. Geosci.* **2010**, *3* (6), 417−421.
(42) Amstaetter, K.; Borch, T.; Kappler, A. Influence of humic acid imposed changes of ferrihydrite aggregation on microbial Fe(III) reduction. *Geochim. Cosmochim. Acta* **2012**, *85* (0), 326−341.
(43) Kappler, A.; Benz, M.; Schink, B.; Brune, A. Electron shuttling via humic acids in microbial iron(III) reduction in a freshwater sediment. *FEMS Microbiol. Ecol.* **2004**, *47* (1), 85−92.
(44) Jiang, J.; Kappler, A. Kinetics of microbial and chemical reduction of humic substances: Implications for electron shuttling. *Environ. Sci. Technol.* **2008**, *42* (10), 3563−3569.
(45) von Canstein, H.; Ogawa, J.; Shimizu, S.; Lloyd, J. R. Secretion of flavins by *Shewanella* species and their role in extracellular electron transfer. *Appl. Environ. Microbiol.* **2008**, *74* (3), 615−623.
(46) Marsili, E.; Baron, D. B.; Shikhare, I. D.; Coursolle, D.; Gralnick, J. A.; Bond, D. R. *Shewanella* secretes flavins that mediate extracellular electron transfer. *Proc. Natl. Acad. Sci. U. S. A.* **2008**, *105* (10), 3968−3973.
(47) Karlsson, T.; Persson, P. Coordination chemistry and hydrolysis of Fe(III) in a peat humic acid studied by X-ray absorption spectroscopy. *Geochim. Cosmochim. Acta* **2010**, *74* (1), 30−40.
(48) Karlsson, T.; Persson, P. Complexes with aquatic organic matter suppress hydrolysis and precipitation of Fe(III). *Chem. Geol.* **2012**, *322*−*323* (0), 19−27.
(49) Mikutta, C. X-ray absorption spectroscopy study on the effect of hydroxybenzoic acids on the formation and structure of ferrihydrite. *Geochim. Cosmochim. Acta* **2011**, *75* (18), 5122−5139.
(50) Eusterhues, K.; Wagner, F. E.; Hausler, W.; Hanzlik, M.; Knicker, H.; Totsche, K. U.; Kogel-Knabner, I.; Schwertmann, U. Characterization of ferrihydrite-soil organic matter coprecipitates by X-ray diffraction and mossbauer spectroscopy. *Environ. Sci. Technol.* **2008**, *42* (21), 7891−7897.
(51) Morup, S.; Ostenfeld, C. W. On the use of Mossbauer spectroscopy for characterisation of iron oxides and oxyhydroxides in soils. *Hyperfine Interact.* **2001**, *136* (1−2), 125−131.
(52) Vanloosdrecht, M. C. M.; Norde, W.; Lyklema, J.; Zehnder, A. J. B. Hydrophobic and electrostatic parameters in bacterial adhesion. *Aquat. Sci.* **1990**, *52* (1), 103−114.
(53) Sparks, D. L., *Environmental Soil Chemistry*. 2nd ed.; Academic Press: Boston, 2002.
(54) Roden, E. E.; Zachara, J. M. Microbial reduction of crystalline iron(III) oxides: Influence of oxide surface area and potential for cell growth. *Environ. Sci. Technol.* **1996**, *30* (5), 1618−1628.
(55) Ekstrom, E. B.; Learman, D. R.; Madden, A. S.; Hansel, C. M. Contrasting effects of Al substitution on microbial reduction of Fe(III) (hydr)oxides. *Geochim. Cosmochim. Acta* **2010**, *74* (24), 7086−7099.
(56) Jones, A. M.; Collins, R. N.; Rose, J.; Waite, T. D. The effect of silica and natural organic matter on the Fe(II)-catalysed transformation and reactivity of Fe(III) minerals. *Geochim. Cosmochim. Acta* **2009**, *73* (15), 4409−4422.
(57) Roden, E. E.; Kappler, A.; Bauer, I.; Jiang, J.; Paul, A.; Stoesser, R.; Konishi, H.; Xu, H. Extracellular electron transfer through microbial reduction of solid-phase humic substances. *Nat. Geosci* **2010**, *3* (6), 417−421.
(58) Bell, P. E.; Mills, A. L.; Herman, J. S. Biogeochemical conditions favoring magnetite formation during anaerobic iron reduction. *Appl. Environ. Microbiol.* **1987**, *53* (11), 2610−2616.
(59) Fredrickson, J. K.; Zachara, J. M.; Kennedy, D. W.; Dong, H. L.; Onstott, T. C.; Hinman, N. W.; Li, S. M. Biogenic iron mineralization accompanying the dissimilatory reduction of hydrous ferric oxide by a groundwater bacterium. *Geochim. Cosmochim. Acta* **1998**, *62* (19−20), 3239−3257.
(60) Zachara, J. M.; Kukkadapu, R. K.; Fredrickson, J. K.; Gorby, Y. A.; Smith, S. C. Biomineralization of poorly crystalline Fe(III) oxides by dissimilatory metal reducing bacteria (DMRB). *Geomicrobiol. J.* **2002**, *19* (2), 179−207.
(61) O'Loughlin, E. J.; Gorski, C. A.; Scherer, M. M.; Boyanov, M. I.; Kemner, K. M. Effects of oxyanions, natural organic matter, and bacterial cell numbers on the bioreduction of lepidocrocite (γ-FeOOH) and the formation of secondary mineralization products. *Environ. Sci. Technol.* **2010**, *44* (12), 4570−4576.
(62) Hansel, C. M.; Benner, S. G.; Fendorf, S. Competing Fe(II)-induced mineralization pathways of ferrihydrite. *Environ. Sci. Technol.* **2005**, *39* (18), 7147−7153.
(63) Piepenbrock, A.; Dippon, U.; Porsch, K.; Appel, E.; Kappler, A. Dependence of microbial magnetite formation on humic substance and ferrihydrite concentrations. *Geochim. Cosmochim. Acta* **2011**, *75* (22), 6844−6858.
(64) Banfield, J. F.; Welch, S. A.; Zhang, H. Z.; Ebert, T. T.; Penn, R. L. Aggregation-based crystal growth and microstructure development in natural iron oxyhydroxide biomineralization products. *Science* **2000**, *289* (5480), 751−754.
(65) Yee, N.; Shaw, S.; Benning, L. G.; Nguyen, T. H. The rate of ferrihydrite transformation to goethite via the Fe(II) pathway. *Am. Mineral.* **2006**, *91* (1), 92−96.
(66) Porsch, K.; Dippon, U.; Rijal, M. L.; Appel, E.; Kappler, A. In-situ magnetic susceptibility measurements as a tool to follow geomicrobiological transformation of Fe minerals. *Environ. Sci. Technol.* **2010**, *44* (10), 3846−3852.
(67) Tronc, E.; Belleville, P.; Jolivet, J. P.; Livage, J. Transformation of ferric hydroxide into spinel by Fe(II) adsorption. *Langmuir* **1992**, *8* (1), 313−319.
(68) Yang, L.; Steefel, C. I.; Marcus, M. A.; Bargar, J. R. Kinetics of Fe(II)-catalyzed transformation of 6-line ferrihydrite under anaerobic flow conditions. *Environ. Sci. Technol.* **2010**, *44* (14), 5469−5475.
(69) Refait, P.; Memet, J. B.; Bon, C.; Sabot, R.; Genin, J. M. R. Formation of the Fe(II)-Fe(III) hydroxysulphate green rust during marine corrosion of steel. *Corros. Sci.* **2003**, *45* (4), 833−845.
(70) Zegeye, A.; Mustin, C.; Jorand, F. Bacterial and iron oxide aggregates mediate secondary iron mineral formation: Green rust versus magnetite. *Geobiol.* **2010**, *8* (3), 209−222.
(71) Hunter, R. C.; Beveridge, T. J. Application of a pH-sensitive fluoroprobe (C-SNARF-4) for pH microenvironment analysis in *Pseudomonas aeruginosa* biofilms. *Appl. Environ. Microbiol.* **2005**, *71* (5), 2501−2510.
(72) Jorand, F.; Zegeye, A.; Ghanbaja, J.; Abdelmoula, M. The formation of green rust induced by tropical river biofilm components. *Sci. Total Environ.* **2011**, *409* (13), 2586−2596.
(73) Roden, E. E.; Urrutia, M. M. Influence of biogenic Fe(II) on bacterial crystalline Fe(III) oxide reduction. *Geomicrobiol. J.* **2002**, *19* (2), 209−251.
(74) Berry, F. J.; Skinner, S.; Thomas, M. F. ^{57}Fe Mossbauer spectroscopic examination of a single crystal of Fe_3O_4. *J. Phys.: Condens. Matter* **1998**, *10* (1), 215−220.

(75) Henneberry, Y. K.; Kraus, T. E. C.; Nico, P. S.; Horwath, W. R. Structural stability of coprecipitated natural organic matter and ferric iron under reducing conditions. *Org. Geochem.* **2012**, *48* (0), 81−89.
(76) Cismasu, A. C.; Michel, F. M.; Tcaciuc, A. P.; Tyliszczak, T.; Brown, G. E. Composition and structural aspects of naturally occurring ferrihydrite. *C. R. Geosci.* **2011**, *343* (2−3), 210−218.
(77) O'Loughlin, E. J.; Kelly, S. D.; Cook, R. E.; Csencsits, R.; Kemner, K. M. Reduction of uranium(VI) by mixed iron(II/iron(III) hydroxide (green rust): Formation of UO_2 nanoparticles. *Environ. Sci. Technol.* **2003**, *37* (4), 721−727.
(78) Larese-Casanova, P.; Scherer, M. M. Abiotic transformation of hexahydro-1,3,5-trinitro-1,3,5-triazine (RDX) by green rusts. *Environ. Sci. Technol.* **2008**, *42* (11), 3975−3981.